Dual Sampling Rate Observer for Motor Position Estimation Using Linear Hall Sensors and Iterative Algorithm

Jonghwa Kim*, Min-Hyun Kim*, Kwanghyun Cho**, and Seibum Choi *
* Korea Advanced Institute of Science and Technology, Daejeon, Korea
** Samsung Electronics, Hwaseong-si, Korea

***Abstract*-- This study suggests a position estimator using linear hall effect sensors and iterative algorithm. Compared to other typical position sensors such as encoders and resolvers, hall effect sensors have several advantages. (e.g., insensitivity to both external disturbances and environmental contaminations, and having a scaleless property). Furthermore, linear hall sensors provide more detailed information on the motor position (i.e., finer resolution) than that of square wave hall sensors. Using those characteristics, a position estimator with linear hall sensors is proposed. Considering the sinusoidal property of the magnetic flux distribution along the position of the motor system, an iterative algorithm with dual sampling rates is applied. The effectiveness of the suggested method was validated with a simulation.**

***Index Terms*—Dual sampling rate observer, Linear hall effect sensor, Position estimation, Scaleless motor system.**

I. Introduction

Nowadays, motor actuated systems are commonly used in many industrial areas for various purposes. The information on the motor position is essential for successful completion of the mission. The most widely used two types of position sensors are optical encoders [1], [2] and resolvers [3], [4]. An optical encoder can provide a finer resolution than that of others; however, it is very sensitive to shock, vibration, oil, moisture, obstacles and dust. Moreover, it requires an additional scale along the required stroke. On the other hand, a resolver is robust against external contaminations. Nevertheless, its application is limited due to its considerable size and weight.

Compared to optical encoders and resolvers, hall effect sensors have strong advantages in terms of weight, size and price. Furthermore, it is scaleless and insensitive to both contaminations and disturbances. Considering the coarse resolution of the square wave hall effect sensors [5], [6] because they detect only the edge signals at the boundaries of permanent magnets, in this study, linear hall effect sensors were used to obtain the position information of a motor system.

Because the linear hall effect sensors detect the magnetic flux distribution along the position of the permanent magnets in a motor system, the measurement mainly consists of a sinusoidal wave for which the period is identical to the length of one permanent magnet pair. However, due to the arrangement pattern of the permanent magnet array, a significant amount of a third order harmonic component is included. Therefore, in this study, the fundamental and third order harmonic components in the hall sensor measurement are taken into account to estimate the motor position. In addition, because it is difficult to extract a unique solution from the summation of sinusoidal functions in a direct way, an iterative algorithm is applied.

The rest of this paper is organized as follows. The design of the position estimating algorithm is discussed in Section II. The dual sampling rate observer is presented in Section III. The convergence proof and performance validation for the suggested method are shown in Section IV and V, respectively. And finally conclusions are given in Section VI.

II. Position Estimator

Even though there exist some other harmonic components with smaller magnitudes in the linear hall sensor measurement due to several reasons, in this study, for the sake of simplicity and as done in some other studies [7], [8], only the fundamental and third order harmonic components were considered. Therefore, the linear hall sensor signal model can be expressed as follows:

$$y = A\sin\left(x + a\right) + B\sin\left(3\left(x + b\right)\right), \qquad (1)$$

where y represents the hall sensor signal, A and B the magnitudes of the fundamental and third order harmonic components, respectively, x the motor position, and a and b the phase of each harmonic component.

However, as briefly mentioned earlier in the previous section, it is difficult to extract a unique and correct solution x against a single y directly in eq. (1). For that reason, the secant method, which is a kind of iterative algorithm, is used as follows:

This work was supported in part by the MSIP (Ministry of Science, ICT and Future Planning), Korea, under the ITRC (Information Technology Research Center) support program (IITP-2016-H8601-16-1005) supervised by the IITP (Institute for Information & communications Technology Promotion), the BK21 plus program, the Technological Innovation R&D program of SMBA (S2341501), and the National Research Foundation of Korea (NRF) grant funded by the Korea government (MSIP) (No.2010-0028680).

$$\hat{x}_n = \hat{x}_{n-1} - \frac{f(\hat{x}_{n-1})}{\dfrac{f(\hat{x}_{n-1}) - f(\hat{x}_{n-2})}{\hat{x}_{n-1} - \hat{x}_{n-2}}}, \qquad (2)$$

where $\hat{x}_n$ is the estimated position at step n. By defining the function f as follows:

$$f(\hat{x}_{n-1}) \triangleq y(\hat{x}_{n-1}) - y_m(x_n), \qquad (3)$$

where y_m is the hall sensor measurement, the position estimate $\hat{x}$ that makes the $f(\hat{x})$ goes to 0 can be obtained through the iteration. A more detailed description for the convergence proof is given in Section IV.

III. Dual Sampling Rate Observer

To guarantee the "iteration" exactly in eq. (2), the hall sensor measurement y_m in f should be held for several steps while the position estimation (iteration) is running. To satisfy this restriction without any performance degradation, a kind of dual sampling rate observer [9] is designed as follows.

The sampling time to update the hall sensor measurement y_m was set 10 times longer than the iteration sampling time for the position estimation. In general, the electrical part (i.e., current controller) is located in the inner loop of the mechanical part (e.g., position or velocity controller). In other words, the current controller operates with a bandwidth 5~10 times faster than that of the position or velocity controller. Therefore, by simply setting the sampling time for the position estimation (i.e., iteration algorithm) identical to the sampling time for the current control, a dual sampling rate observer is achievable without any hardware upgrade or significant increase in computational burden. Fig. 1 describes these dual sampling times. In Fig. 1, k_1 and k_2 represent the step number for the hall sensor measurement update and the iteration loop, respectively. k_1 is a monotonically increasing integer; however, k_2 is a repeating integer from 0 to 9 shown in Fig. 1. Therefore, the time t can be expressed as a function of k_1 and k_2 as follows:

$$t = f(k_1, k_2) = Tsm * k_1 + Tsc * k_2. \qquad (4)$$

IV. Convergence Proof

In this section, the convergence property of the iterative algorithm suggested in the previous sections is verified by the following two divisions.

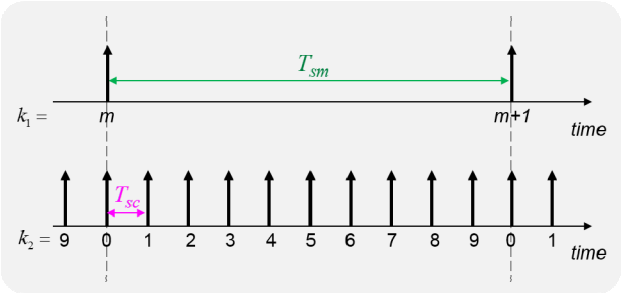

Fig. 1. Dual sampling times (*Tsm*: sampling time for measurement update; *Tsc*: sampling time for the iteration)

A. Measurement hold $(k_2 = 1 \sim 9)$

First, the period when the hall sensor measurement is held (i.e., $k_2 = 1 \sim 9$) is considered. By combining with eq. (3) and using eq. (4), eq. (2) can be rewritten as eq. (5). Because the hall sensor measurement is being held, the two y_m terms in eq. (5) cancel each other out. Therefore,

$$\hat{x}_{k_1,k_2} = \hat{x}_{k_1,k_2-1} - \frac{y(\hat{x}_{k_1,k_2-1}) - y_m(x_{k_1,k_2})}{\dfrac{y(\hat{x}_{k_1,k_2-1}) - y(\hat{x}_{k_1,k_2-2})}{\hat{x}_{k_1,k_2-1} - \hat{x}_{k_1,k_2-2}}}. \qquad (6)$$

By assuming that the sampling time is small enough, the hall sensor signal model y is continuous, and the inclination angle of the signal model y around the position x can be defined as α, eq. (6) can be rewritten as follows:

$$\hat{x}_{k_1,k_2} = \hat{x}_{k_1,k_2-1} - \frac{y(\hat{x}_{k_1,k_2-1}) - y_m(x_{k_1,k_2})}{\alpha}. \qquad (7)$$

Meanwhile, in finding the approximate solution for an equation such as

$$x = g(x) \qquad (8)$$

using following numerical method

$$\hat{x}_n = g(\hat{x}_{n-1}), \qquad (9)$$

The following theorem guarantees the convergence property.

Theorem: Let $g:[a,b] \to [a,b]$ *be a differentiable function such that* $|g'(x)| \le \gamma < 1$ *for all* $x \in [a,b]$. *Then g has exactly one fixed point* l_0 *in* $[a,b]$, *and the sequence* (x_n) *with a starting point* $x_0 \in [a,b]$ *converges to* l_0.

Differentiation of the right hand side of eq. (7) with respect to position x is calculated as follows:

$$g'(x) = 1 - \frac{y'(x)}{\alpha} \approx 0. \qquad (10)$$

$$\hat{x}_{k_1,k_2} = \hat{x}_{k_1,k_2-1} - \frac{y(\hat{x}_{k_1,k_2-1}) - y_m(x_{k_1,k_2})}{\dfrac{\left\{y(\hat{x}_{k_1,k_2-1}) - y_m(x_{k_1,k_2})\right\} - \left\{y(\hat{x}_{k_1,k_2-2}) - y_m(x_{k_1,k_2-1})\right\}}{\hat{x}_{k_1,k_2-1} - \hat{x}_{k_1,k_2-2}}} \qquad (5)$$

$$\hat{x}_{k_1+1,0} = \hat{x}_{k_1,9} - \frac{y(\hat{x}_{k_1,9}) - y_m(x_{k_1+1,0})}{\frac{\left\{y(\hat{x}_{k_1,9}) - y_m(x_{k_1+1,0})\right\} - \left\{y(\hat{x}_{k_1,8}) - y_m(x_{k_1,0})\right\}}{\hat{x}_{k_1,9} - \hat{x}_{k_1,8}}} \tag{11}$$

The aforementioned assumption was used again in eq. (10), and from the theorem expressed above, the iterative algorithm of eq. (2), therefore, converges at least as long as the hall sensor measurement is being held.

B. *Measurement update* $(k_2 = 0)$

At the time of the hall sensor measurement update, eq. (2) can be rewritten as eq. (11). Because the approximate solution (i.e., estimated position) converges through the iterations as discussed in the previous section for the *'Measurement hold'* period, the following equations are applicable:

$$\left|y(\hat{x}_{k_1,9}) - y(\hat{x}_{k_1,8})\right| \approx 0 \tag{12}$$

or

$$\left|y(\hat{x}_{k_1,9}) - y(\hat{x}_{k_1,8})\right| \ll \left|y_m(x_{k_1+1,0}) - y_m(x_{k_1,0})\right| \tag{13}$$

and

$$y(\hat{x}_{k_1,9}) \approx y_m(x_{k_1,0}) \ . \tag{14}$$

By applying the above equations, the following equation is obtained:

$$\hat{x}_{k_1+1,0} \approx \hat{x}_{k_1,9} \ . \tag{15}$$

Therefore, the estimated position information is held during the hall sensor measurement update, and from the next step on (i.e., $k_2=1$), it will start again to converge to the new updated value.

V. Performance Validation

In this section, the performance of the position estimator suggested in this paper is validated through a simulation. The system parameters for the simulation are shown in Table I.

TABLE I
SYSTEM PARAMETERS FOR THE SIMULATION

Parameter	Value	Unit
Sampling time for the iteration (Tsm)	0.5	ms
Sampling time for the measurement update (Tsc)	50	μs
Coefficient for the fundamental harmonic component (A)	0.6	
Coefficient for the third order harmonic component (B)	0.06	
Phase for the fundamental harmonic component (a)	0	
Phase for the third order harmonic component (b)	0	

Referencing [10], the magnitude ratio of the third order harmonic component to the fundamental harmonic component was set to 0.1. In addition, for simplicity, the phases for the harmonic components were set to zero, and the hall sensor measurement was assumed to be sensed under a constant traveling speed of 6π rad/s. The hall sensor modeling error was set to 3% of the original magnitude, and sensor measurement noise was considered.

The simulation results are shown in Fig. 2 and Fig. 3. In Fig. 2, the position estimation error at every final iteration step (i.e., $k_2=9$) is plotted. Fig. 2 convincingly shows the effectiveness of the suggested method for the motor position estimation. Fig. 3 shows the position estimation error along the iteration while the sensor measurement is held (i.e., $k_2=1\sim9$) and updated ($k_2=0$). As can easily be seen in Fig. 3, the convergence property along the iteration is also verified. In this case, two times of iteration were enough for the saturation. However, a certain amount of steady state error exists due to the difference between the model and the real value, which was assigned by 3%, and measurement noise. The RMS and maximum position estimation error by suggested method are summarized in Table II.

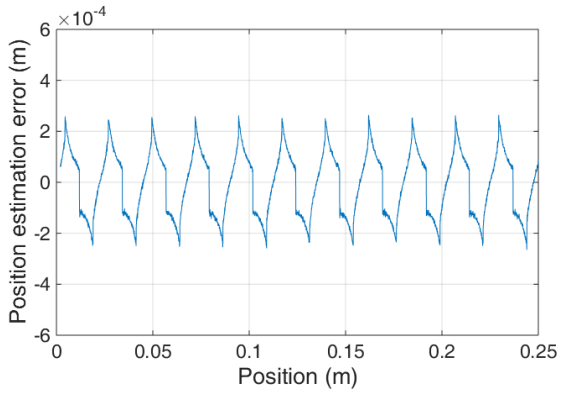

Fig. 2. Position estimation error at each final iteration step *($k_2=9$)*

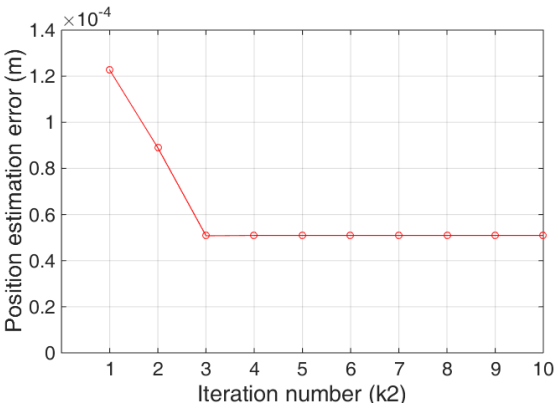

Fig. 3. Position estimation error along the iteration *($k_2=1\sim10$)*

TABLE II
RMS AND MAX. POSITION ESTIMATION ERROR

	Value	Unit
RMS error	0.13052	mm
Max. error	0.26571	mm

VI. CONCLUSIONS

In this paper, a dual sampling rate observer was developed for motor position estimation using linear hall sensors and an iterative algorithm. The position estimating algorithm itself is not complicated. Furthermore, no additional hardware upgrade or computational burden is required for the suggested dual sampling rate algorithm. The convergence property along the iteration was also proven mathematically. Finally, the possibility of a better position estimation through the dual sampling rates and iteration was verified by the simulation results. However, in real systems, the hall sensor measurement has further harmonic components. Therefore, the exact performance of the suggested method and algorithm should be validated by actual experiments under various conditions.

REFERENCES

[1] K. Cho, J. Kim, S. Choi and S. Oh, "A High-Precision Motion Control Based on a Periodic Adaptive Disturbance Observer in a PMLSM," *IEEE/ASME Trans. Mechatronics,* vol. 20, no. 5, pp. 2158-2171, Oct. 2015.

[2] J. Kim, K. Cho and S. Choi, "Lumped Disturbance Compensation using Extended Kalman Filter for Permanent Magnet Linear Motor System," *Int. J. Control Autom. Syst.,* to be published, DOI: 10.1007/s12555-014-0400-1.

[3] C. Attaianese, G. Tomasso, "Position Measurement in Industrial Drives by Means of Low-Cost Resolver-to-Digital Converter," *IEEE Trans. Instrum. Meas.*, vol. 56, no. 6, pp. 2155-2159, Dec. 2007.

[4] R. Hoseinnezhad, A. Bab-Hadiashar, P. Harding, "Calibration of Resolver Sensors in Electromechanical Braking Systems: A Modified Recursive Weighted Least-Squares Approach," *IEEE Trans. Ind. Electron.*, vol. 54, no. 2, pp. 1052-1060, Apr. 2007.

[5] S. Morimoto, M. Sanada, Y. Takeda, "High-performance current-sensorless drive for PMSM and SynRM with only low-resolution position sensor," *IEEE Trans. Ind. Appl.,* vol. 39, no. 3, pp. 792-801, May/June 2003.

[6] Y. Yang and Y. Ting, "Improved angular displacement estimation based on hall-effect sensors for driving a brushless permanent-magnet motor," *IEEE Trans. Ind. Electron.,* vol. 61, no. 1, pp. 504-511, Jan. 2014.

[7] S. Jung and K. Nam, "PMSM control based on edge-field hall sensor signals through ANF-PLL processing," *IEEE Trans. Ind. Electron.,* vol. 58, no. 11, pp. 5121-5129, Nov. 2011.

[8] H. A. Toliyat, L. Hao, D. S. Shet and T. A. Nondahl, "Position-sensorless control of surface-mount permanent-magnet AC (PMAC) motors at low speeds," *IEEE Trans. Ind. Electron.,* vol. 49, no. 1, pp. 157-164, Feb. 2002.

[9] L. Kovudhikulrungsri, "Discrete-Time Observer with Dual Sampling Rates and its Applications to Drive Control with Wide Speed Range," *Ph.D. dissertation, Dept. Elect. Eng., Tokyo Univ.,* Tokyo, Japan, 2004

[10] J. Kim, S. Choi, K. Cho and K. Nam, "Position Estimation Using Linear Hall Sensors for Permanent Magnet Linear Motor Systems," *IEEE Trans. Ind. Electron..,* to be published, DOI: 10.1109/TIE.2016.2591899.